

# A SEARCH FOR RADIO GRAVITATIONAL LENSES, USING THE SLOAN DIGITAL SKY SURVEY AND THE VERY LARGE ARRAY

EDWARD R. BOYCE<sup>1</sup>, JUDD D. BOWMAN, ADAM S. BOLTON, JACQUELINE N. HEWITT AND SCOTT BURLES  
Massachusetts Institute of Technology, Department of Physics and Kavli Institute for Astrophysics and Space Research, 77  
Massachusetts Avenue, Cambridge MA 02139

*Draft version November 5, 2018*

## ABSTRACT

We report on a novel search for radio gravitational lenses. Using the Very Large Array, we imaged ten candidates with both dual redshifts in Sloan Digital Sky Survey spectra and 1.4 GHz radio flux  $\geq 2$  mJy in the FIRST survey. The VLA maps show that in each case the radio emission is associated with the foreground galaxy rather than being lensed emission from the background galaxy, although at least four of our targets are strong lenses at optical wavelengths. These SDSS dual-redshift systems do not have lensed radio emission at the sensitivity of current radio surveys.

*Subject headings:* gravitational lensing — galaxies: elliptical and lenticular, cD — galaxies: starburst

## 1. INTRODUCTION

Strong gravitational lenses have long been recognized for their unique ability to constrain the mass distributions of galaxies. There over 100 currently known lenses (Muñoz et al. 1999; Browne et al. 2003), most of which have been discovered as bright quasars that show multiple images surrounding a faint lensing galaxy. Although this is a sizable number of lenses, it is a significant limiting factor for the statistical study of galaxy properties, thus the identification of new lenses remains an important ongoing effort. Compounding the challenges of studying galaxy properties through lensing is that it is often difficult to acquire the requisite photometry, redshifts, and internal kinematics of the lens galaxies themselves due to the selection effects created by identifying lenses from bright images.

The Sloan Digital Sky Survey (SDSS; York et al. (2000)) is providing new opportunities to search for gravitational lenses in an information rich environment. The photometry and spectroscopy available for all SDSS objects means that detected lens galaxies automatically have redshifts, kinematics and photometry. Efforts have been underway for several years to exploit the SDSS archive in combination with other resources, such as the HST, that have had considerable success identifying several new lenses (Bolton et al. 2005; Oguri et al. 2004, 2005; Pindor et al. 2004; Johnston et al. 2003; Inada et al. 2003; Morgan et al. 2003).

Among these projects is a unique sample of spectroscopically selected lens candidates from SDSS compiled by Bolton et al. (2004). This sample has led to the discovery of several new lenses (Bolton et al. 2005; Bolton & Burles 2005) and has the distinct advantage that any confirmed lens system has known lens and source redshifts as well as an optically bright lens galaxy.

Radio lenses, in which a radio bright source is lensed by a radio dim lens, are an interesting subset of gravitational lenses. In this paper we describe an exploratory effort to utilize the SDSS archive and the FIRST radio

catalog (Becker et al. 1995) to provide a bridge from optically selected lens candidates to viable radio candidates. By correlating sources in the FIRST catalog with the spectroscopically selected sample of SDSS galaxies of Bolton et al. (2004) and additional similar galaxies, targets emerge that exhibit both radio emission and dual redshifts in optical spectra. If the radio emission is from the background object, there is a high probability of lensing.

The use of these two surveys together has been proposed as a possible method to reduce the candidate list for gravitational lens surveys by future radio telescopes such as the Square Kilometer Array (SKA) that should be able to detect large numbers of faint radio lenses (Bowman et al. 2004).

## 2. LENSING CANDIDATES

We started with a sample of 117 gravitational lens candidates drawn from the SDSS luminous red galaxy (LRG) sample (Eisenstein et al. 2001) and absorption-dominated spectra of the main galaxy sample (Strauss et al. 2002). These are massive red galaxies which should act as effective gravitational lenses. Candidates were assigned a redshift in the range 0.15-0.65 by the specBS software (Schlegel et al. 2005).

A search procedure using a matched filter method found spectra with nebular emission lines at higher redshift than that of the red galaxy (Bolton et al. 2004). This method detects the emission line [OII] $\lambda\lambda 3727$  at  $S/N > 3$ , and at least two of the emission lines H $\beta\lambda 4861$ , O[III] $\lambda 4959$  and O[III] $\lambda 5007$  at  $S/N > 2.5$ , all at the same redshift. These emission lines are generated in nebulae around young massive stars (age  $< 20$  Myr), when ultraviolet radiation from the young stars is absorbed shortward of the Lyman limit and re-emitted at optical wavelengths. Nebular emission lines are strong in galaxies with many young stars and a high star formation rate (Kennicutt 1998). The presence of at least three emission lines indicates that a higher redshift star-forming galaxy lies near the red galaxy, probably within the 3'' SDSS fiber. If the impact parameter is small enough, gravitational lensing may occur. Our sample, including the 49 LRG candidates from Bolton et al. (2004) and 68 additional candidates from the main galaxy sample, is

Electronic address: eboyce@mit.edu, jdbowman@mit.edu, bolton@mit.edu, jhewitt@space.mit.edu, burles@mit.edu

<sup>1</sup> National Radio Astronomy Observatory, PO Box O, 1003 Lopezville Road, Socorro NM 87801

TABLE 1  
SDSS PROPERTIES OF OUR LENS CANDIDATES.

Candidate	$z_{FG}$	$z_{BG}$	$\sigma_v$ (km/s)	$\Delta\theta$ (")
SDSS J003753.21-094220.1	0.1955	0.6322	$279 \pm 10$	2.94
SDSS J073728.44+321618.6	0.3223	0.5812	$338 \pm 16$	2.67
SDSS J081323.37+451809.4	0.1834	0.6435	$237 \pm 13$	2.20
SDSS J095629.78+510006.3	0.2405	0.4700	$334 \pm 15$	2.94
SDSS J113629.47-022303.9	0.3936	0.4646	$321 \pm 27$	0.81
SDSS J120540.43+491029.3	0.2150	0.4807	$235 \pm 10$	1.62
SDSS J130613.65+060022.1	0.1730	0.4722	$242 \pm 17$	2.04
SDSS J140228.22+632133.3	0.2046	0.4814	$267 \pm 17$	2.23
SDSS J155030.75+521759.8	0.4564	0.5388	$345 \pm 52$	0.92
SDSS J225125.87-092635.8	0.4719	0.6238	$414 \pm 47$	2.09

NOTE. — The properties of our lens candidates as inferred from the SDSS spectra.  $z_{FG}$  is the redshift of the foreground red galaxy,  $z_{BG}$  is the redshift of the emission lines superimposed on the galaxy spectrum and  $\sigma_v$  is the velocity dispersion of the foreground galaxy.  $\Delta\theta = 8\pi(\sigma_v^2/c^2)(D_{LS}/D_S)$  is the separation of the two lensed images in a singular isothermal sphere model with the measured  $\sigma_v$ , and gives an expected angular scale for gravitational lensing.

the subject of many follow-up observations to determine which candidates are lenses.

To find radio lens candidates, we cross matched the 117 candidates with the 1.4 GHz FIRST radio survey (Becker et al. 1995), and found that 13 candidates were within 1".5 of a FIRST source. The FIRST radio emission may have been associated with either the foreground red galaxy or the background star-forming galaxy. In the latter case, the foreground galaxy may lens the background emission.

The FIRST survey has angular resolution 4", and so FIRST images cannot show lensing morphologies on a scale of 1-2". We made radio observations at higher angular resolution to look for evidence of lensing, as described in the following section. We selected nine candidates with a FIRST flux greater than 2.0 mJy and excluded three candidates below this flux limit. J0037-0942 is known to be a lens from optical integral field spectroscopy, and we included this known lens although its FIRST flux is 1.39 mJy. Table 1 lists the sample of ten candidates, giving the full SDSS names. For the remainder of the paper, we abbreviate the names. Note that lens image separations for an isothermal sphere model are calculated from the redshifts and foreground galaxy velocity dispersions, giving an expected scale for lensing in the system.

### 3. OBSERVATIONS

The ten candidates were observed in 8.4 GHz continuum mode with the NRAO Very Large Array (VLA) on 2004 October 7 and 2004 November 7. The VLA was in A configuration, giving angular resolution 0".24 (Taylor et al. 2004). The observations were intended to detect multiple lensed components, with double lenses being detectable up to a flux ratio of 10:1. The total 8.4 GHz flux was estimated from the 1.4 GHz flux in the FIRST survey, assuming a radio galaxy spectral index  $S_\nu \propto \nu^{-0.5}$ . The integration time for each target was set to detect at the  $5\sigma$  level a component with 1/11 of the estimated flux, and varied from 9 to 72 minutes. Details of the observations are given in Table 2.

The data were flagged, calibrated and imaged in AIPS,

TABLE 2  
RADIO OBSERVATIONS OF THE LENS CANDIDATES.

Candidate	$\nu$ (GHz)	rms ( $\mu$ Jy/beam)
J0037-0942	8.4	19
J0037-0942	4.9	26
J0037-0942	1.4	71
J0737+3216	8.4	38
J0813+4518	8.4	34
J0956+5100	8.4	33
J1136-0223	8.4	15
J1205+4910	8.4	16
J1306+0600	8.4	16
J1402+6321	8.4	19
J1550+5217	8.4	39
J2251-0926	8.4	20

NOTE. — The observing frequency and rms noise (measured from the maps) for each of our targets.

following standard procedures. Maps were made with pixel sizes of  $\sim 0''.065$ , with slight variations depending on declination. J0813+4518 and J0956+5100 only showed low brightness emission, and therefore these maps (Figures 5 and 6) were not deconvolved. All other sources were deconvolved using the CLEAN algorithm.

Two components were seen in the 8.4 GHz maps of J0037-0942, and it was initially thought that the source might be a lens. Additional VLA time was available due to a gap in the schedule, and on 2004 November 10 this system was observed for 44 minutes at 4.9 GHz and for 20 minutes at 1.4 GHz. These maps (Figures 2 and 3) have angular resolutions of 0".4 and 1".4, respectively (Taylor et al. 2004).

### 4. RESULTS

Strong gravitational lensing of a background point source generates two or four bright images, offset from the position of the background object. Two bright images form on either side of the foreground lens galaxy, or four bright images form in a ring around the lens galaxy. If the background source is extended then the images may appear as tangential arcs. The separation of two bright images or the diameter of a ring of images should be close to the separations predicted for an isothermal sphere model, as given in Table 1. The 8.4 GHz VLA maps were examined for multiple or ring-like components that would be generated by gravitational lensing.

Lens images should be offset from the foreground galaxy by about half the expected lens image separation given in Table 1, typically 0".5-1".0. The sizes and relative positions of radio components have errors of 0".12, equal to half the 0".24 angular resolution of the VLA maps. In matching radio components to the foreground galaxy we also consider the resolution of SDSS and the absolute astrometry of both systems. For the VLA maps we used phase calibrators with A or B positional accuracy codes, giving absolute astrometry accurate to 0".1 (Perley & Taylor 2003). SDSS objects have absolute astrometric errors up to 0".105 (Pier et al. 2003), while we conservatively assume a 0".1 error in measuring the centroid of the foreground galaxy, as the centroiding algorithms differ by up to this amount (Pier et al. 2003). Adding these

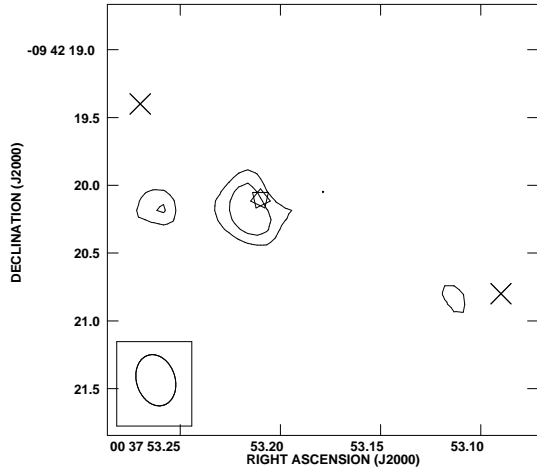


FIG. 1.— 8.4 GHz VLA map of J0037-0942. The star marks the centroid of the foreground red galaxy, the crosses mark the optical lens images. VLA contours are set at  $(-3, 3, 5) \times 19 \mu\text{Jy beam}^{-1}$ .

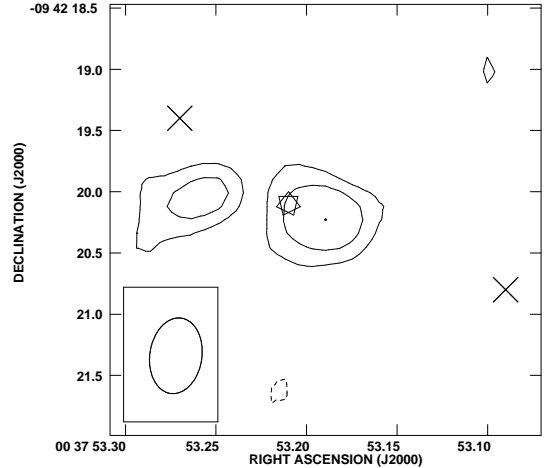


FIG. 2.— 4.9 GHz VLA map of J0037-0942. The star marks the centroid of the foreground red galaxy, the crosses mark the optical lens images. VLA contours are set at  $(-3, 3, 5, 8) \times 26 \mu\text{Jy beam}^{-1}$ . Note that the resolution of this map is  $0''.4$ .

four errors in quadrature gives an overall error of  $0''.2$  in the registration of radio components to the centroid of the SDSS red galaxy. If lensing occurs, an offset of at least  $0''.5$  between the foreground galaxy and the lensed images should be obvious.

J0037-0942 was initially considered as a gravitational lens, although we have now concluded that the radio flux is not lensed (see below). The remaining nine targets are clearly not lenses on the basis of the radio morphology. The radio maps do not show separate sources either side of the foreground galaxy, or a ring of emission around the galaxy. The radio emission is peaked at or very near the location of the foreground galaxy, and sometimes shows the lobes typical of radio galaxies. The following sections discuss the individual sources in detail.

#### 4.1. J0037-0942

J0037-0942 was initially considered as a lens, as it has two separate components (Figures 1, 2 and 3). The components are  $0''.7 \pm 0''.1$  apart at 8.4 GHz,  $1''.0 \pm 0''.2$  apart at 4.9 GHz, and blended together in the low resolution 1.4 GHz map. The stronger component overlaps the foreground galaxy, appearing slightly to the east of it at 8.4 GHz and slightly to the west at 4.9 GHz. The weaker component appears to the east of the foreground galaxy, and shifts slightly to the north at 4.9 GHz. The increased separation at 4.9 GHz relative to 8.4 GHz indicates a varying spectral index, with both components having steeper spectral indices on their outer edges.

As the peak of the radio emission overlaps the red galaxy, and the radio components are much closer together than the predicted lens image separation of  $2''.9$  (Table 1), we conclude that the radio flux is generated by the foreground object and is not lensed emission from the background star-forming galaxy. The source has a bright core near the center and a weaker lobe  $0''.7-1''.0$  to the east (a projected distance 2-3 kpc<sup>2</sup>).

J0037-0942 is a gravitational lens at optical wavelengths, based on integral field spectroscopy (Bolton &

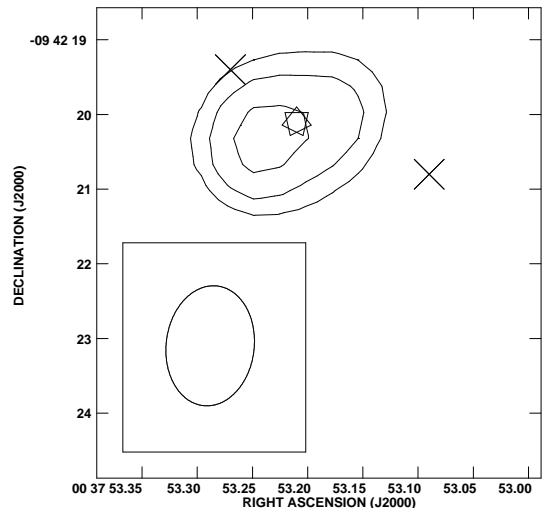


FIG. 3.— 1.4 GHz VLA map of J0037-0942. The star marks the centroid of the foreground red galaxy, the crosses mark the optical lens images. VLA contours are set at  $(-3, 3, 5, 8) \times 71 \mu\text{Jy beam}^{-1}$ . Note that the resolution of this map is  $1''.4$ .

Burles 2005). Narrow-band images at the redshifted emission line wavelengths show two images of the background star-forming galaxy,  $3''.0$  apart and either side of the foreground red galaxy (the image positions are shown by crosses in Figures 1, 2 and 3). The optical lens images are at very different positions to the radio components and have a much larger separation. The considerable difference between the optical morphology and the radio morphology strengthens the case that the radio emission comes from the foreground galaxy.

#### 4.2. J0737+3216

The VLA map shows a point source  $0''.1 \pm 0''.2$  from the SDSS position (Figure 4). There is no evidence for multiple components and the radio emission overlaps the foreground galaxy. We conclude that the radio flux is not lensed emission from the background galaxy. The foreground galaxy appears to host a radio source with

<sup>2</sup> We assume a  $\Lambda$ CDM cosmology with  $H_0 = 70 \text{ km/s}$ ,  $\Omega_m = 0.3$ ,  $\Omega_\Lambda = 0.7$  throughout

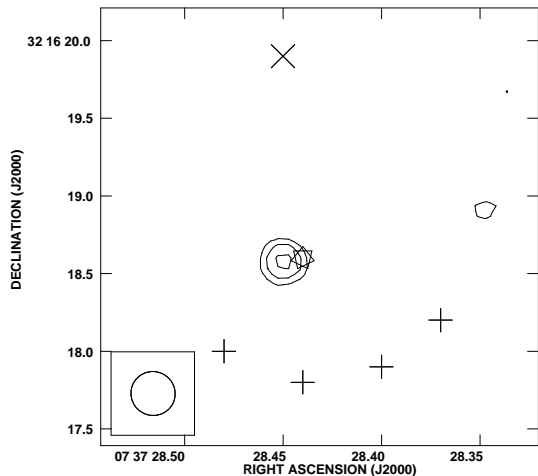


FIG. 4.— 8.4 GHz VLA map of J0737+3216. The star marks the centroid of the foreground red galaxy, the cross marks the optical lens point image, the plus signs trace the optical lens arc image. VLA contours are set at  $(-3, 3, 5, 8) \times 38 \mu\text{Jy beam}^{-1}$ .

projected size  $< 1.1$  kpc.

J0737+3216 is a gravitational lens at optical wavelengths, based on integral field spectroscopy (Bolton & Burles 2005). Narrow-band images at the redshifted emission line wavelengths show two images of the background star-forming galaxy around the foreground red galaxy, a point on one side and a tangential arc on the other (the image positions are shown by crosses and plus signs in Figure 4). None of the images is near the radio point source. The extreme difference between the optical morphology and the radio morphology strengthens the case that the radio emission comes from the foreground galaxy.

#### 4.3. J0813+4518

The VLA map shows a roughly linear structure extended over  $2''.0 \pm 0''.1$ , with a peak at the SDSS position (Figure 5). Although the size matches the expected lensing scale of  $2''.2$  (Table 1), the continuous linear morphology is not characteristic of lensing and the peak of the emission overlaps the foreground galaxy. We conclude that the radio flux is not lensed emission from the background galaxy. The foreground galaxy appears to be a radio galaxy with a projected size  $6.2 \pm 0.3$  kpc.

#### 4.4. J0956+5100

The VLA map shows a roughly linear structure extended over  $0''.8 \pm 0''.1$ , with a peak at the SDSS position (Figure 6). The size is much less than the predicted lensing scale of  $2''.9$  (Table 1), the continuous linear morphology is not characteristic of lensing and the peak of the emission overlaps the foreground galaxy. We conclude that the radio flux is not lensed emission from the background galaxy. The foreground galaxy appears to be a radio galaxy with a projected size  $\sim 3.0 \pm 0''.4$  kpc.

J0956+5100 is a gravitational lens at optical wavelengths, based on integral field spectroscopy (Bolton & Burles 2005). Narrow-band images at the redshifted emission line wavelengths show two images of the background star-forming galaxy either side of the foreground

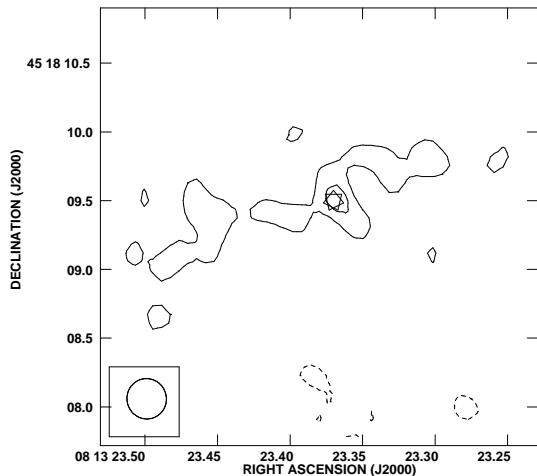


FIG. 5.— 8.4 GHz VLA map of J0813+4518. The star marks the centroid of the foreground red galaxy. VLA contours are set at  $(-3, 3, 5) \times 34 \mu\text{Jy beam}^{-1}$ .

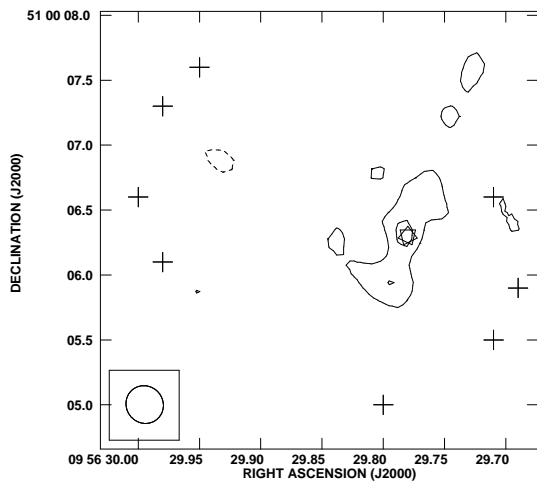


FIG. 6.— 8.4 GHz VLA map of J0956+5100. The star marks the centroid of the foreground red galaxy, the plus signs trace the optical lens arc images. VLA contours are set at  $(-3, 3, 5) \times 33 \mu\text{Jy beam}^{-1}$ .

red galaxy, each stretched into a tangential arc (the image positions are shown by plus signs in Figure 6). Neither lens arc is close to the linear radio source. The extreme difference between the optical morphology and the radio morphology strengthens the case that the radio emission comes from the foreground galaxy.

#### 4.5. J1136-0223

The VLA map shows a linear double structure with peaks  $0''.5 \pm 0''.1$  apart, either side of the SDSS position (Figure 7). The peak separation is not much less than the predicted lens image separation of  $0''.8$  (Table 1), but the continuous linear morphology is not characteristic of lensing. We conclude that the radio flux is not lensed emission from the background galaxy. The foreground object appears to be a radio galaxy with projected linear size  $2.7 \pm 0.5$  kpc.

#### 4.6. J1205+4910

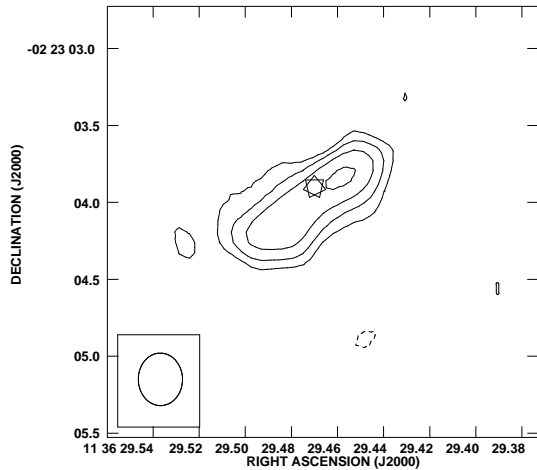


FIG. 7.— 8.4 GHz VLA map of J1136-0223. The star marks the centroid of the foreground red galaxy. VLA contours are set at  $(-3, 3, 5, 8, 13) \times 15 \mu\text{Jy beam}^{-1}$ .

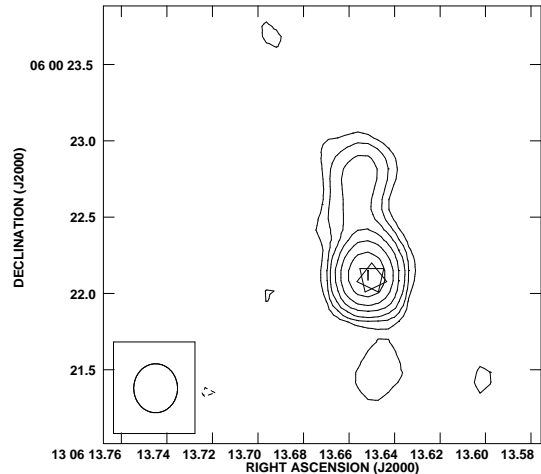


FIG. 9.— 8.4 GHz VLA map of J1306+0600. The star marks the centroid of the foreground red galaxy. VLA contours are set at  $(-3, 3, 5, 8, 13, 21, 34, 55) \times 16 \mu\text{Jy beam}^{-1}$ .

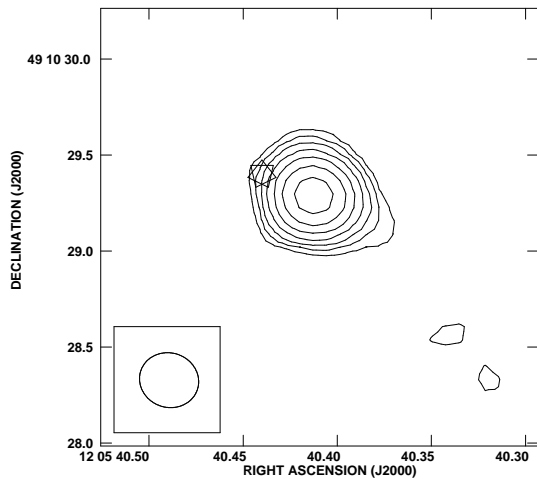


FIG. 8.— 8.4 GHz VLA map of J1205+4910. The star marks the centroid of the foreground red galaxy. VLA contours are set at  $(-3, 3, 5, 8, 13, 21, 34, 55) \times 16 \mu\text{Jy beam}^{-1}$ .

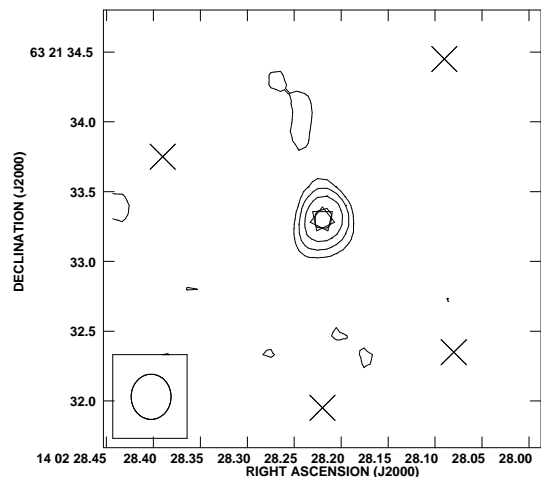


FIG. 10.— 8.4 GHz VLA map of J1402+6321. The star marks the centroid of the foreground red galaxy, the crosses mark the optical lens images.  $(-3, 3, 5, 8, 13) \times 19 \mu\text{Jy beam}^{-1}$ .

The VLA map shows an unresolved  $1.24 \pm 0.03$  mJy source  $0''.4 \pm 0''.2$  west of the center of the foreground galaxy (Figure 8). No other component is detected to a limit  $0.08$  mJy ( $5\sigma$  noise limit of the map). If the system were an asymmetric lens, then the next brightest image would be more than 15 times fainter than the brightest image. Faint images form closer to the foreground galaxy than the brightest image, so the images would be  $< 1''$  apart. Since the expected separation of lens images for this system is  $1''.6$  (Table 1), J1205+4910 is not an asymmetric lens. It is likely that the foreground red galaxy is a radio galaxy with a bright lobe  $1.4 \pm 0.7$  kpc from its center in projection. Given the offset between the radio and optical positions, we may even be seeing a radio source at a third redshift.

#### 4.7. J1306+0600

The VLA map shows a triple source with a strong central peak overlapping the SDSS position. There is extended emission leading to a secondary peak to the north and another peak to the south (Figure 9). The separa-

tion of the peaks is  $1''.3 \pm 0''.1$ , as opposed to an expected lensing scale of  $2''.0$  (Table 1), and the linear morphology is not characteristic of lensing; we conclude that the radio flux is not lensed emission from the background galaxy. The foreground galaxy appears to be a radio galaxy with projected size  $3''.8 \pm 0''.3$ .

#### 4.8. J1402+6321

The VLA map shows a strong unresolved source at the SDSS position, with faint extended emission  $1''.0 \pm 0''.1$  to the north (Figure 10). Lens images are predicted to have a much larger separation of  $2''.2$  (Table 1) and the strong emission peak at the location of the foreground object is not characteristic of lensing. We conclude that the radio flux is not lensed emission from the background galaxy. The foreground galaxy appears to host a radio galaxy with a central core of projected size  $< 0.8$  kpc, and a weak lobe extending north to a projected distance  $3.4 \pm 0.3$  kpc.

J1402+6321 is a gravitational lens at optical wave-

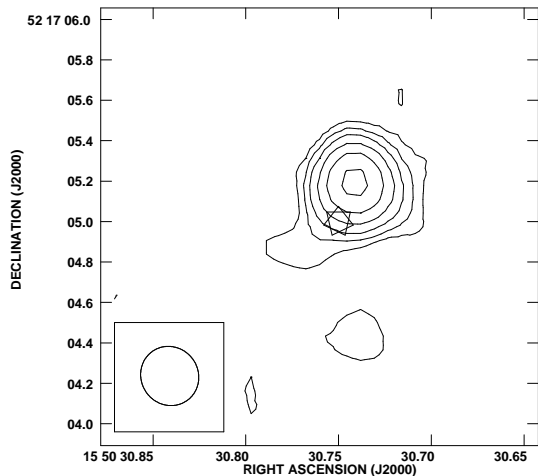


FIG. 11.— 8.4 GHz VLA map of J1550+5217. The star marks the centroid of the foreground red galaxy. VLA contours are set at  $(-3, 3, 5, 8, 13, 21, 34) \times 39 \mu\text{Jy beam}^{-1}$ .

lengths, based on integral field spectroscopy and Hubble Space Telescope imaging (Bolton et al. 2005). Narrow-band images at the redshifted emission line wavelengths show four images of the background star-forming galaxy around the foreground galaxy (the image positions are shown by crosses in Figure 10). None of the lens images is near the radio point source. The extreme difference between the optical morphology and the radio morphology strengthens the case that the radio emission comes from the foreground galaxy.

#### 4.9. J1550+5217

The VLA map shows a strong peak  $0''.2 \pm 0''.2$  north of the SDSS position, with a faint extension through the center of the red galaxy, and a weak component  $0''.8 \pm 0''.1$  south of the strong peak (Figure 11). Although the components have a separation similar to the  $0''.9$  predicted for lensing (Table 1), the strong emission peak overlapping the foreground object is not characteristic of lensing. We conclude that the radio flux is not lensed emission from the background galaxy. The foreground galaxy appears to host a radio galaxy, with total projected size  $4.6 \pm 0.6$  kpc.

Bolton & Burles (2005) have made integral field observations of this system. It seems likely that there is no lensing in the optical regime either, although the integral field data are inconclusive.

#### 4.10. J2251-0926

The VLA map shows an unresolved  $1.14 \pm 0.04$  mJy source  $0''.5 \pm 0''.2$  northwest of the center of the foreground galaxy (Figure 12). No other component is detected to a limit 0.1 mJy ( $5\sigma$  noise limit of the map). If the system were an asymmetric lens, then the next brightest image would be more than 11 times fainter than the brightest image. Faint images form closer to the foreground galaxy than the brightest image, and the images would be  $< 1''$  apart. Since the expected separation of lens images for this system is  $2''.1$  (Table 1), J2251-0926 is not an asymmetric lens.

The foreground galaxy appears to be the cD galaxy of a  $z = 0.47$  galaxy cluster, as six smaller galaxies are seen

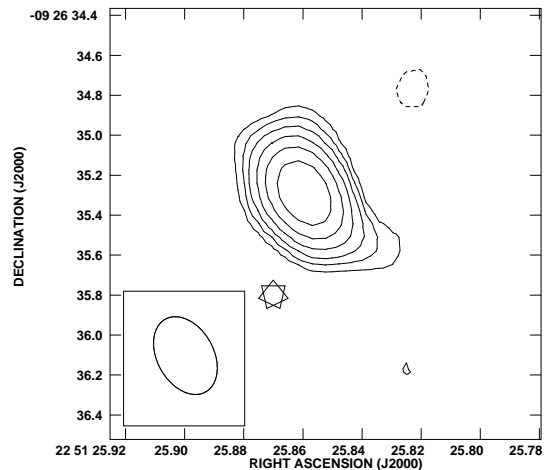


FIG. 12.— 8.4 GHz VLA map of J2251-0926. The star marks the centroid of the foreground red galaxy. VLA contours are set at  $(-3, 3, 5, 8, 13, 21, 34) \times 20 \mu\text{Jy beam}^{-1}$ .

in SDSS within  $15''$ . Lensing by a cluster with velocity dispersion up to 1000 km/s could produce two images separated by up to  $12''$ , with the radio source near the central foreground galaxy being the fainter image. However no other radio source is detected within  $20''$  in our 8.4 GHz VLA map (with a limiting flux 0.1 mJy) or the FIRST survey (with a limiting 1.4 GHz flux of 0.75 mJy); the cluster lens explanation is also rejected.

It is likely that the foreground galaxy is a radio galaxy, with a bright lobe  $3.0 \pm 1.2$  kpc from its center in projection. Given the offset between the radio and optical positions, we may even be seeing a radio source at a third redshift.

## 5. CONCLUSIONS

Nine of the 117 candidate massive red galaxy lenses, or 8%, have a 1.4 GHz flux  $S_{1.4} \geq 2.0$  mJy in the FIRST survey, and in each case we attribute the radio emission to the foreground galaxy. We consider the probability that this many galaxies would exceed our flux limit due to their intrinsic radio luminosity.

The SDSS Data Release 3 includes 36,551 luminous red galaxies (LRGs) with  $0.15 < z < 0.65$ . We take these massive galaxies to be similar to our lens candidate sample (some of our candidates were in the LRG sample, others were massive galaxies in the main sample but not the LRG sample). 2,255 of the 36,551 LRGs, or 6.2%, have  $S_{1.4} \geq 2.0$  mJy in FIRST. Most of these do not lens a background object, so the radio emission is generated by the LRG itself. We assume a binomial distribution with a 6.2% probability for each lens candidate to have intrinsic  $S_{1.4} \geq 2.0$  mJy. There is a 30% probability that at least nine of 117 candidates would exceed the flux limit due to their own radio emission. It is entirely probable that the detected radio flux could come from the foreground object in all of our candidates.

Conversely, it would be difficult to observe radio emission from the background star-forming galaxies. We assume that the background galaxies do not have active galactic nuclei (AGN), as these would likely have been apparent in the SDSS spectrum. Galaxies without an AGN have 1.5 GHz luminosity  $\leq 2 \times 10^{23} \text{WHz}^{-1}$  (Fig. 3

of Condon (1992)). For a typical case, a  $z = 0.5$  galaxy with 1.5 GHz luminosity  $2 \times 10^{21} \text{WHz}^{-1}$ , the 1.5 GHz flux would be  $2 \mu\text{Jy}$  before lensing and 10-20  $\mu\text{Jy}$  after a lensing magnification of a few. Current radio surveys such as FIRST have detection limits of  $\sim 10^3 \mu\text{Jy}$  (Becker et al. 1995), so radio sources selected from these surveys are unlikely to be lensed images of star-forming galaxies. Future radio telescopes such as the Square Kilometer Array might detect radio lensed images of star-forming galaxies, although radio emission from the foreground galaxy is likely to be detected as well. The situation will be analogous to optical lensing, where the foreground lens and images of the background object are both seen, and must be disentangled.

Imaging and integral field spectroscopy of SDSS dual redshift systems often confirm strong lensing of the optical emission (Bolton et al. 2004, 2005; Bolton & Burles 2005). As an example, five of our ten targets have integral field data (J0037-0942, J0737+3216, J0956+5100, J1402+6321 and J1550+5217, see Section 4), and four of these objects are gravitational lenses at optical wavelengths. The dual optical redshifts automatically select detectable optical emission at different locations along the line of sight, making lensing probable. Continuum radio emission from the more distant object is probably too faint to be detected with current instruments, so lensed radio emission need not be detected.

Our sample of ten gravitational lens candidates revealed no radio lenses. In each case the radio emission was associated with the nearby red galaxy, rather than the more distant star-forming galaxy. Identification of dual redshift systems in SDSS red galaxy spectra is an excellent method for detecting strong galaxy-galaxy lensing of optical emission. However these SDSS dual redshift systems are unlikely to be detected in current radio surveys, and the few strong radio sources are located in

foreground galaxies rather than lensed background galaxies.

Support for this work was provided by the National Science Foundation through grant AST 00-71181.

The National Radio Astronomy Observatory is a facility of the National Science Foundation operated under cooperative agreement by Associated Universities, Inc.

Funding for the creation and distribution of the SDSS Archive has been provided by the Alfred P. Sloan Foundation, the Participating Institutions, the National Aeronautics and Space Administration, the National Science Foundation, the U.S. Department of Energy, the Japanese Monbukagakusho, and the Max Planck Society. The SDSS Web site is <http://www.sdss.org/>.

The SDSS is managed by the Astrophysical Research Consortium (ARC) for the Participating Institutions. The Participating Institutions are The University of Chicago, Fermilab, the Institute for Advanced Study, the Japan Participation Group, The Johns Hopkins University, the Korean Scientist Group, Los Alamos National Laboratory, the Max-Planck-Institute for Astronomy (MPIA), the Max-Planck-Institute for Astrophysics (MPA), New Mexico State University, University of Pittsburgh, University of Portsmouth, Princeton University, the United States Naval Observatory, and the University of Washington.

We would like to thank NRAO Staff, particularly Meri Stanley and Ken Hartley, who greatly assisted EB in the preparation of the VLA observing schedule at very short notice.

We would like to thank the anonymous referee, whose comments improved this paper considerably.

Facilities: NRAO(VLA), SDSS.

#### REFERENCES

- Becker, R. H., White, R. L., & Helfand, D. J. 1995, *ApJ*, 450, 559  
 Bolton, A. S., Burles, S., Schlegel, D. J., Eisenstein, D. J. & Brinkmann, J. 2004, *AJ*, 127, 1860  
 Bolton, A. S., Burles, S., Koopmans, L. V. E., Treu, T. & Moustakas, L. A. 2005, *ApJ*, 624, L21  
 Bolton, A. S. & Burles, S. 2005, in preparation  
 Bowman, J. D., Hewitt, J. N., & Kiger, J. R. 2004, *ApJ*, 617, 81  
 Browne, I. W. A., et al. 2003, *MNRAS*, 341, 13  
 Condon, J. J. 1992, *ARA&A*, 30, 575  
 Eisenstein, D. J., et al. 2001, *AJ*, 122, 2267  
 Inada, N., et al. 2003, *AJ*, 126, 666  
 Johnston, D. E., et al. 2003, *AJ*, 126, 2281  
 Kennicutt, R. C. 1998, *ARA&A*, 36, 189  
 Morgan, N. D., Snyder, J. A., & Reens, L. H. 2003, *AJ*, 126, 2145  
 Muñoz, J. A., Falco, E. E., Kochanek, C. S., Lehar, J., McLeod, B. A., Impey, C. D., Rix, H.-W. & Peng, C. Y. 1999, *Ap&SS*, 263, 51  
 Oguri, M., et al. 2005, *ApJ*, 622, 106  
 Oguri, M., et al. 2004, *PASJ*, 56, 399  
 Perley, R. A., & Taylor, G. B. 2003, *VLA Calibration Manual* (Socorro: NRAO), <http://www.aoc.nrao.edu/~gtaylor/calib.html>  
 Pier, J. R., Munn, J. A., Hindsley, R. B., Hennessy, G. S., Kent, S. M., Lupton, R. H., & Ivezić, Z. 2003 *AJ*, 125, 1559  
 Pindor, B. et al., 2004, *AJ*, 127, 1318  
 Richards, G. T., et al. 2004, *AJ*, 127, 1305  
 Schlegel, D.J., et al. 2005, in preparation  
 Strauss, M. A., et al. 2002, *AJ*, 124, 1810  
 Taylor, G. B., Ulvestad, J. A., & Perley, R. A. 2004, *The Very Large Array Observational Status Summary* (Socorro: NRAO), <http://www.vla.nrao.edu/astro/guides/vlas/current/>  
 York, D. G., et al. 2000, *AJ*, 120, 1579